Recent poleward shift of tropical cyclone formation and its link to tropical expansion

S. Sharmila[*,1], K. J. E. Walsh[1]

[1]*School of Earth Sciences, University of Melbourne, Australia*

*Corresponding author

S. Sharmila

School of Earth Sciences

University of Melbourne, Victoria, Australia 3010.

Email: sharmila.climate@gmail.com

Submitted to Nature Climate Change

8 Jan 2018

Abstract.

Recent research indicates that the annual-mean locations of tropical cyclones (TCs) are migrating towards higher latitudes in recent decades, concurring with the observed expansion of the tropics induced by anthropogenic global warming. However, the causal linkage between poleward movement of TC genesis (TCG) and recent observed tropical expansion remains unexplored. Here, we investigate how large-scale dynamical effects combined with coherent changes in the regional Hadley circulation (HC) evidently explain the recent changes in regional TCG and its poleward movement over most of the ocean basins. We show that the recent upper-level weakening of the rising branch of the HC in the deep tropics, partly induced by the increased vertical stability, has likely suppressed the low-latitude TCG in most ocean basins via anomalous large-scale subsidence. The regional variations in the HC have also favoured a poleward displacement of TC-favourable climate conditions through a warming-induced poleward shift of the HC's meridional extent, followed by a poleward migration of TCG in recent times. Our results provide a new basis for inferring the contribution of global warming in modulating future TC estimates via the climate pathway of tropical expansion.

Keywords: Tropical cyclone genesis, poleward migration, tropical expansion, Hadley circulation, global warming

Main.

Tropical cyclones (TCs) are among the most catastrophic of high-impact weather events and have triggered substantial mortality and huge economic damage over the populated tropical coastal regions in recent decades[1]. Since the life-cycle of TCs is critically sensitive to large-scale tropical climate conditions[2,3], the observed increases in the sea surface temperatures (SST) over tropical ocean basins in recent decades[4,5] attributed to anthropogenic global warming[6] are expected to complicate the status and fate of TC genesis (TCG) around the globe through gradual modification of TC-favourable tropical environments[7,8]. Despite increasing research efforts, the issue of how regional-scale TCG has changed or will change in the context of global warming remains controversial and challenging[6,9,10]. An improved understanding of the underlying warming-induced climatic factors and relevant physical mechanisms that have regulated the regional-scale TCG in recent decades is therefore crucial to benchmark future TC estimates.

Recent research[11] indicates that the observed annual-mean locations where TCs reach their lifetime-maximum intensity (LMI) are systematically migrating poleward in most regions in the last 30 years, concurrent with marked changes in the TC-favourable large-scale climate conditions. A follow-up modelling study[12] projected continuing poleward shift of LMI over the western north Pacific in a warmer climate. Many previous modelling studies[13,14] also argued that global warming could lead to shifts in TC pathways, although the regional-scale projections remain largely ambiguous[4,15]. A recent study[16] has extended the previous work of Kossin *et al.*[11] for observed TCG locations. With some degree of uncertainty, this study noted a comparable displacement of annual-mean TCG locations, linked with sub-tropical displacement of TC-favourable conditions as measured by potential genesis indices[17,18] (an empirical tool based on a suite of large-scale climate conditions used to identify the potential TC activity) over the Pacific basins during the same period as Kossin's study. These results demonstrate potentially increased threats to locations at higher latitudes that have not been historically prone to TC-related hazards. However, the physical processes that have triggered

such a migration remain unclear. No direct association with the El Niño-Southern Oscillation (ENSO), the dominant mode of tropical climate variability, has been established[11,16]. Kossin and coauthors[11,12] anticipated that such a poleward migration could possibly be linked with the independent expansion of the tropical belt observed since 1980, caused by anthropogenic warming[19]. However, the possible key mechanisms that link the warming-induced observed tropical expansion with large-scale climate factors known to modulate TCG, and their poleward displacement in recent decades, have yet to be elucidated.

The expansion of the tropics is related to the characteristics of the thermally driven tropical mean meridional overturning circulation, also known as the Hadley circulation (HC), a crucial factor for various climatic feedbacks across the globe. Recent evidence[19,20] indicates that the HC is expanding and the zones of sub-tropical descending branch are progressively shifting poleward since 1980. Apart from stratospheric ozone depletion[21], the HC expansion is responsive to anthropogenic climate change[22, 23], while increasing atmospheric stability is predicted to slow down the HC in a warmer climate[24, 25, 26]. Since the attribution of any global warming impact on regional-scale TCG is complex and still controversial, a systematic understanding of the warming-induced behavioural changes in regional-scale HC in close association with TC-favourable large-scale climate conditions in the recent period will therefore provide a useful perspective for estimates of future TC activity.

In this article, we provide a new insight into the causal linkages between observed regional HC and the changing nature of TCG including its meridional displacement in a recent 35-year period (1980-2014). Here, we maximize the relationship between the HC and TCG by examining 'peak' TC seasons (during which >70% of TCs form basin-wise) of individual TC active ocean basins (Supplementary Fig 1). The data used, climate parameters and methods are described in the Methods section.

Figure 1 | Relationship between tropical SST anomaly and atmospheric dry static stability (deep tropics) and annual TCG frequency in recent 35 years.

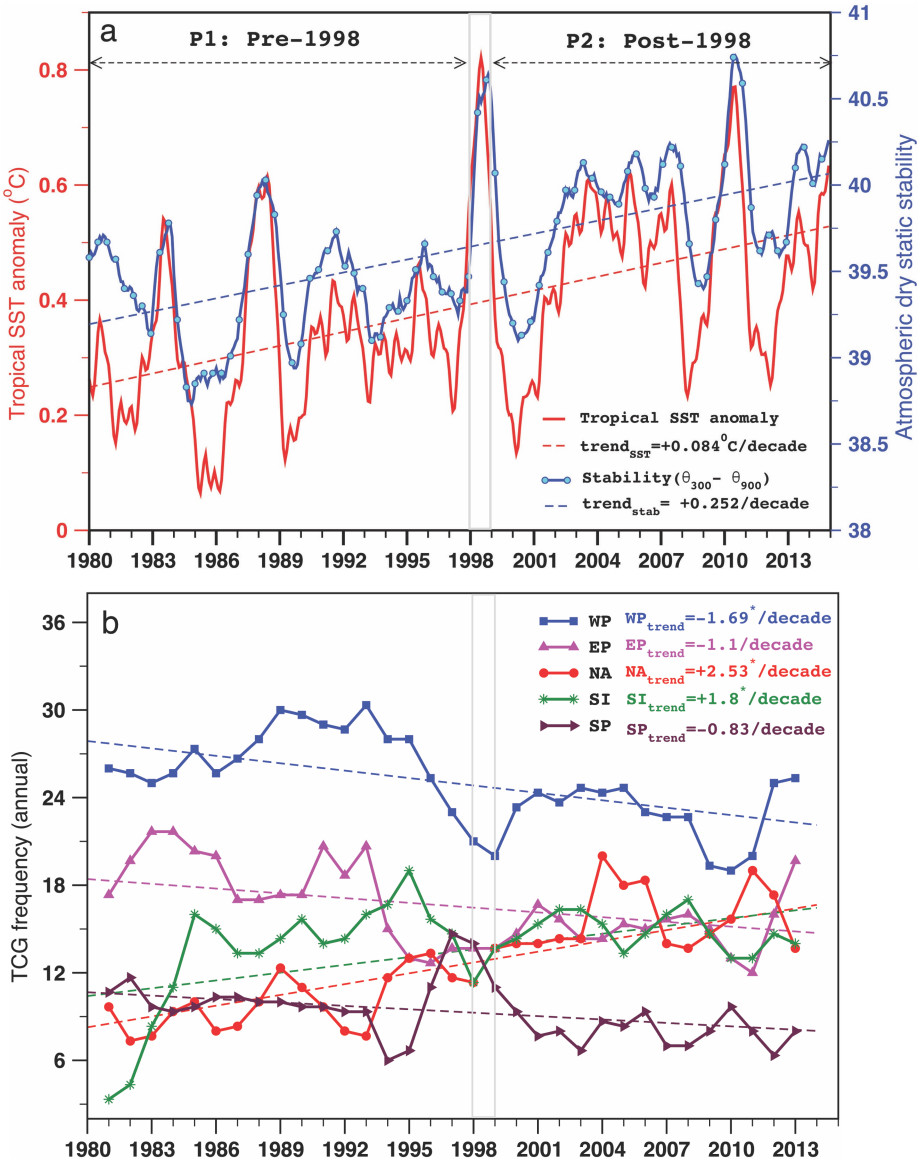

a monthly time series of SST anomaly (ERSST[36] 11-month running mean, red curve) averaged over tropical domain (23.5°N-23.5°S, all longitudes) with respect to the base period 1951-1979. The year 1998 is separated with a box. The mean value tropical SST change ($\Delta\overline{SST}_{P2\text{-}P1}$=+0.11°C) is significant at 95% confidence level. The atmospheric dry static stability (blue curve, potential temperature θ difference between two vertical levels: $\theta_{300} - \theta_{900}$) averaged over deep tropics (10°S-10°N) based on ERA-Interim reanalysis[33]. The correlation (r=0.87) between them is statistically significant (95% confidence level). **b** annual TCG frequency (two-year running mean, solid curves) over Western Pacific (WP; blue), Eastern Pacific (EP; magenta), North Atlantic (NA; red), South Indian Ocean (SI; yellow), and South Pacific (SP; maroon) ocean basins based on the latest IBTrACS[31] data and their corresponding linear trends (dash lines, * indicates significant at p<0.05) calculated for period 1980-2014.

85 The tropical SST anomalies (Fig. 1a; red curve) show a significant warming trend (~+0.25°C
86 from 1980 to 2014) under a general trend of global warming[4], and the mean tropical SST change
87 ($\Delta\overline{SST}$) between the pre- and post-1998 epochs is positive (+0.11°C). Interestingly, a similar
88 increasing trend in the atmospheric dry static stability (defined as the difference of potential
89 temperatures between upper and lower vertical levels) is also evident over the deep tropics (10°S-
90 10°N) (Fig. 1a; blue curve), well correlated (r=0.87) with the recent tropical SST change. Such
91 increasing atmospheric stability appears to agree with the observed warming trend of the tropical
92 upper troposphere[27,28], and thus is potentially important for future estimates. Within this recent period,
93 the latest IBTrACS best-track[29] records indicate a considerable decreasing trend in basin-wide annual
94 TCG frequency over the Pacific (significant in the western north Pacific, -1.69/decade), while a
95 significant increasing trend is observed over the north Atlantic (+2.53/decade), and the south Indian
96 (+1.8/decade) oceans (Fig 1b).

Table 1: Annual and seasonal means of tropical cyclone genesis (TCG) frequency for the period (1980-2014), pre-1998 (P1:1980-1997), post-1998 (P2:1999-2014), and the recent change (P2 - P1).

The values statistically significant at 0.05 and 0.1 levels are marked with * and ** (asterisks) respectively.

	1980-2014	P1(1980-1997)	P2(1999-2014)	ΔP: (P2-P1)	Rel. change (%)
a. Annual					
WP (western Pacific)	25.0	27.28	23.0	-4.28*	-15.7%
EP (eastern Pacific)	16.57	17.78	15.44	-2.34**	-13.2%
NA (north Atlantic)	12.46	9.89	15.25	+5.36*	+54.2%
SI (south Indian)	13.43	12.5	14.56	+2.06**	+16.5%
SP (south Pacific)	9.34	10.06	8.25	-1.81**	-18.0%
b. Peak Season					
WP (JASO)	17.23	18.5	16.19	-2.31*	-12.5%
EP (JAS)	1.49	12.78	10.25	-2.53*	-19.8%
NA (ASO)	8.43	6.44	10.44	+3.99*	+61.0%
SI (JFM)	8.63	8.17	9.31	+1.15**	+14.1%
SP (JFM)	6.97	7.05	6.56	-0.49	-7.0%

97 During the post-1998 period, the peak seasonal TCG frequency has significantly reduced over
98 the western north Pacific and eastern north Pacific, but greatly enhanced over the North Atlantic
99 (Table 1). This begs the question of whether there are differences in the relationship between these
100 trends and climate variables between the basins.
101 When the meridional distributions of observed TCG (Fig. 2a-e) are calculated for individual
102 ocean basins, a considerable reduction in TCG is observed over the Pacific Ocean basins during the
103 post-1998 period, while an increase is seen over the north Atlantic and south Indian basins.
104 Interestingly, a clear poleward shift in the peak genesis distribution is also evident over the main
105 development regions (~10-20° latitudes) among basins during the post-1998 period, indicating a
106 tendency towards low-latitude reduction and poleward increase in TCG frequency in the recent epoch.
107 Here, the use of TCG estimates during peak seasons is noteworthy, compared to the previously noted
108 inconsistency in the latitudinal trends in the annual-average quantities[16]. To better support this global
109 signature of poleward shift of TCGs (except the north Atlantic), we estimated the probability density
110 functions of the relative TCG latitude preference (in %) (Fig. 2f-j) for both the epochs. This
111 normalized analysis has the advantage of removing changes in total numbers and thereby better
112 demonstrating the relative location changes (%) in TCG latitudinal distribution. The relative changes
113 in the maximum probability of TCG latitude preference (in %) have well captured the latitudes of
114 peak variation in TCG frequency as noted in Fig. 2a-e. The histograms clearly indicate a robust and
115 systematic reduction of low-latitude TCG (~5-12° latitudes) along with a coherent poleward shift in
116 the locations of genesis preference during the post-1998 period (red bars) compared to the pre-1998
117 epoch (blue bars) over most of the basins. Note that the histogram has captured a poleward shift in
118 the maximum low-latitude TCG preference (from 12.5°N to 15°N) over the North Atlantic (Fig. 2h)
119 to some extent, compared to Fig. 2c. To illustrate the precise link of dynamical and thermodynamical
120 climate conditions with the systematic reduction at low-latitudes and consequent poleward migration
121 of TCG, we compared the relative meridional changes (%) in vertical wind shear (VWS), and

maximum potential intensity[30] (MPI) during peak TC seasons (Figs. 2k-o) based on ERA-Interim Reanalysis[31], as these variables have been shown to contribute in the observed poleward migration of annual-mean LMI in recent decades[11].

Figure 2 | Epochal changes in TCG and large-scale climate conditions as a function of latitude over the five major ocean basins.

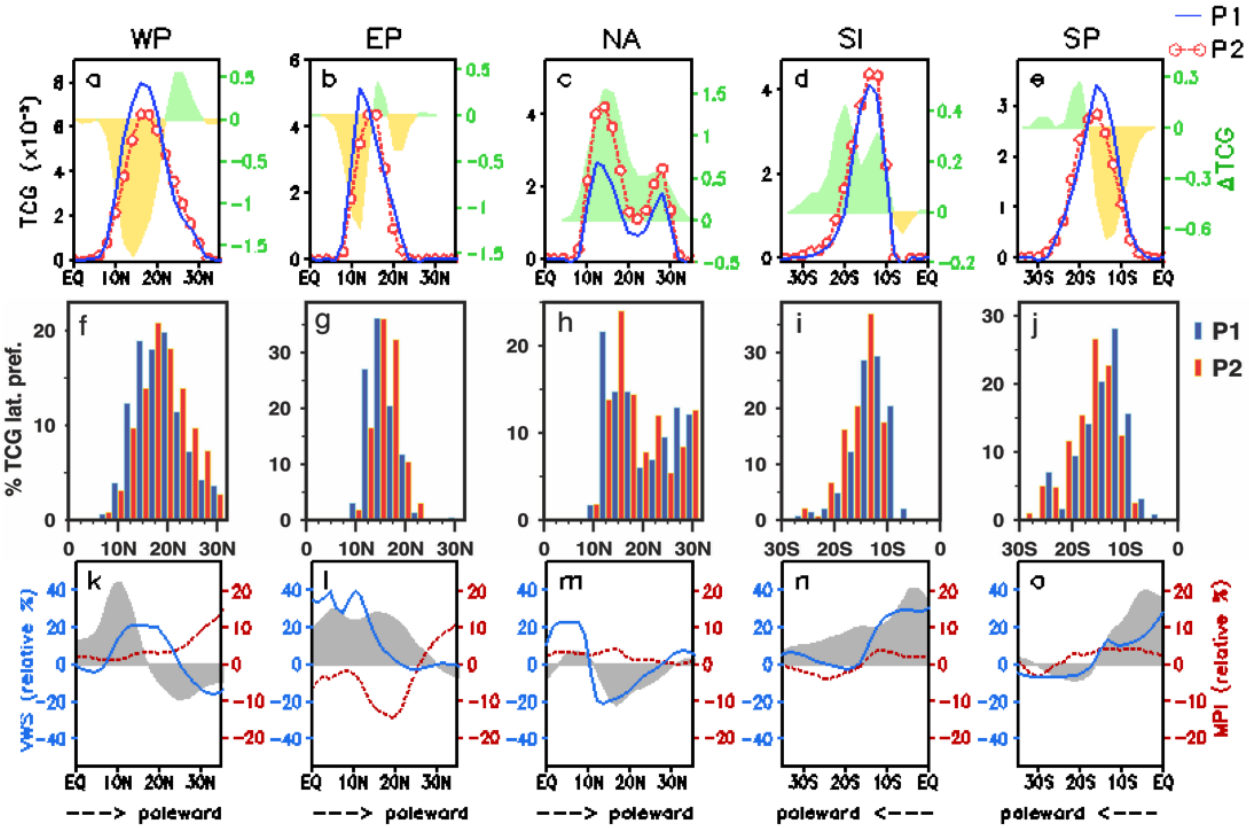

a-e, composite meridional distributions of TCG frequency (per 2°×2° latitude–longitude grid box per season per year) averaged over the individual longitudinal domains of each ocean basins for the pre-1998 (P1; blue) and post-1998 (P2; red) period and their epochal changes (ΔTCG=P2-P1; shaded). **f-j**, probability density histograms of TCG latitude preference (in percentage) relative to total number of TCG per individual ocean basins. **k-o**, relative changes ($\frac{P2-P1}{P1}\times100\%$) in vertical wind shear (VWS; blue) and maximum potential intensity (MPI; red) along with the convective stability (VMS; right Y axis) in grey shades.

Both the frequency and meridional displacement of TCG during post-1998 are in close agreement with the substantial (~10-40%) relative increase (decrease) in VWS (blue curve) at lower

(higher) latitudes during peak TC seasons over all basins, supporting its dominant role in changing basin-wise TCG frequency[10]. In contrast, the variation in local MPI (red curve) is low and not uniformly consistent among basins, indicating a secondary role for local thermodynamical effects. Interestingly, the estimated vertical moist stability (VMS; grey shaded) based on the vertical moist static energy, appears to be intimately tied with the epochal changes in TCG. The VMS shows a robust ~10-30% relative increase coexisting with the low-latitude locations of reduced TCG the recent period. Such increased convective stability over the deep tropics are partly driven by the increased trend in the vertical stability (Fig. 1a), along with the abrupt increase in the low-level vertical stability (Supplementary Fig. 2) closely tied with increasing trend of upper-level moisture content (Supplementary Fig. 3). Such stabilization in the deep tropics can cause distinct dynamical effects, and is expected to influence the strength and meridional extent of the global HC in the recent period. Note that the enhanced TCG over the north Atlantic is concomitant with the decreased VMS and associated weaker VWS over the main development region, indicating a clear basin-dependent difference. A recent modelling study[32] demonstrated that increasing convective stability even in a narrow band around the equator under global warming can account for a major part of the poleward shift of storm tracks in tandem with a poleward expansion of the global HC. Therefore, it is crucial to understand how the regional TCG variations during the post-1998 period, concomitant with the large-scale dynamical effects, are systematically related to the observed tropical expansion.

As the global HC varies with the seasonal cycle, we focus on two main seasons, JAS (July to September) and JFM (January to March), during which the majority of the northern and southern hemispheric TCs form respectively. Figure 3 compares the global mean meridional HC for pre-1998, post-1998, and their epochal changes during JAS and JFM respectively, diagnosed by the streamfunction (ψ) (See Methods). Here, the positive (negative) ψ denotes a clockwise (anticlockwise) circulation, and thus a weakening of large-scale HC corresponds to a positive (negative) value of change in ψ for JAS (JFM). As indicated by the epochal difference (Figs. 3c and

152 3f), meridionally bifurcated but weakened at the upper levels of the ascending branch of the global
153 HC over the deep tropics is clearly seen in both seasons during the post-1998 period significant at the
154 95% confidence level.

Figure 3 | Observed streamfunction (ψ) of the zonal-mean meridional overturning circulation.

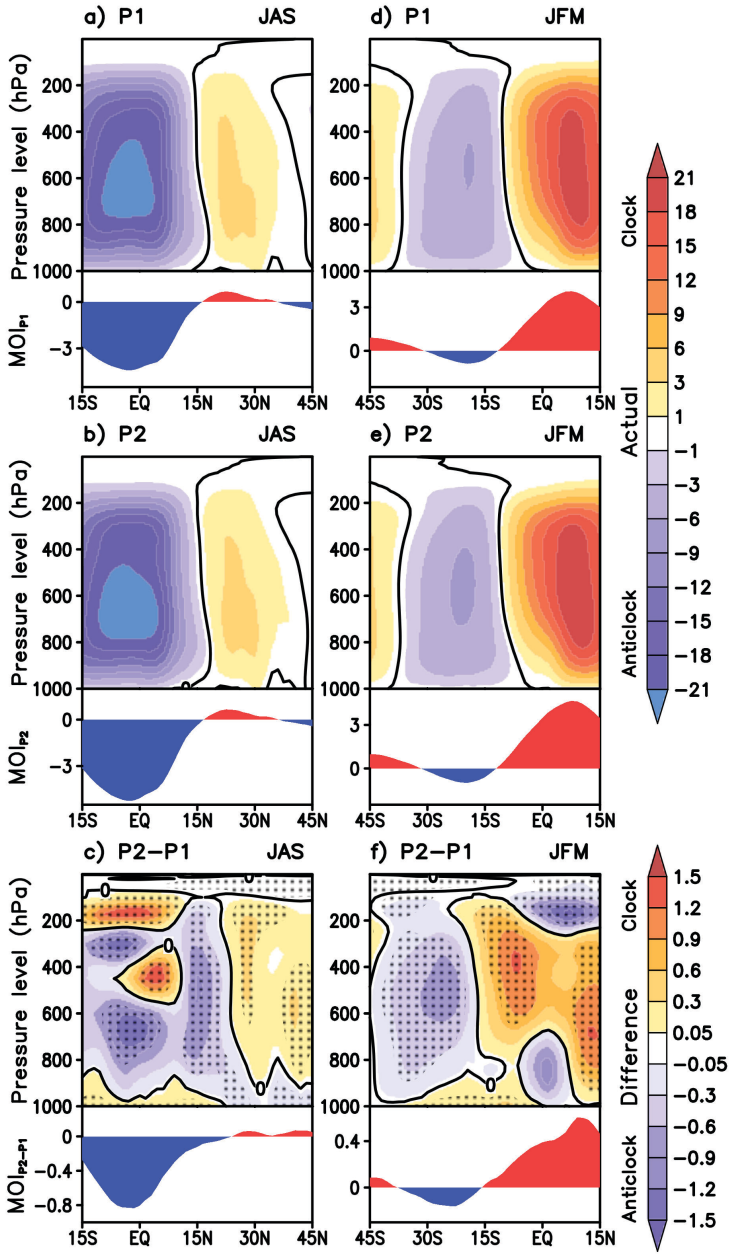

a-c, pre-1998 period (P1), post-1998 period (P2) and recent change (P2-P1) for the boreal summer (JAS). **d-f**, same but during boreal winter (JFM). The positive (negative) value of ψ represents clockwise (anti-clockwise) circulation in the latitude-pressure coordinate. The values significant above 95% confidence level are marked with black dots. The corresponding zonal-mean divergent meridional overturning index

(MOI: $v_{\phi 200} - v_{\phi 850}$) values are also shown at the bottom of each panel. The positive (negative) values shown in red (blue) represents the clockwise (anticlockwise) meridional overturning circulation.

This weakening of the rising branch at the upper level may be linked with the increasing vertical stability shown in Figs. 1b and 2k-o. A robust warming-induced poleward displacement of the large-scale HC is apparent, concomitant with a poleward extension of the sub-tropical dry zones during the post-1998 period, consistent with the observed trends in previous studies[19]. Similar poleward shifts of the global HC are projected to continue through the 21st century as estimated by an ensemble of Coupled Model Intercomparison Project phase 5 (CMIP5) climate models[33] under anthropogenic warming conditions (Supplementary Fig 4), however, the climate models project a widespread weakening of the global HC in a future warmer climate. Furthermore, a close correspondence between epochal changes in the meridional edges of the global Hadley cell and the changes in zonally averaged divergent meridional wind vertical shear (vertical difference between 200 and 850 hPa divergent meridional wind) is also well captured (Fig. 3, bottom panel) for both the seasons, indicating the efficacy of the zonally averaged vertical profile of divergent meridional wind in representing the HC.

Note that the assumption of a non-divergent meridional circulation based on ψ is not valid over limited or regional TCG domains as while the mass is conserved globally, it is not conserved regionally (see Methods). To overcome this limitation, we use the vertical profile of divergent meridional wind and vertical pressure velocity over the regional domains to depict the regional HC over the individual basins (Fig. 4). The observed broader in latitude ascending branch of the regional HC over the western north Pacific, south Pacific, and south Indian basins, along with the narrowing of this branch over the Eastern Pacific and the North Atlantic, and their corresponding descending branches during peak TC seasons are well depicted in Fig. 4. An anomalous large-scale subsidence is evident at ~5º-12º latitudes in the western north Pacific, eastern north Pacific and north Atlantic basins, almost collocated with the reduced low-latitude TCG over most of the basins during the post-1998 period, consistent with Fig. 3. Such a regional tendency towards weakening of the ascending

178 branch of the regional HC shows a close association with the increased vertical wind shear and
179 convective stability in the deep tropics accompanied by a poleward shift of the meridional extent
180 (Figs. 2k-o), in general agreement with the poleward shift in large-scale TC-favourable climate
181 conditions.

Figure 4 | Meridional-vertical structure of the regional Hadley circulation during peak TC seasons over individual basins.

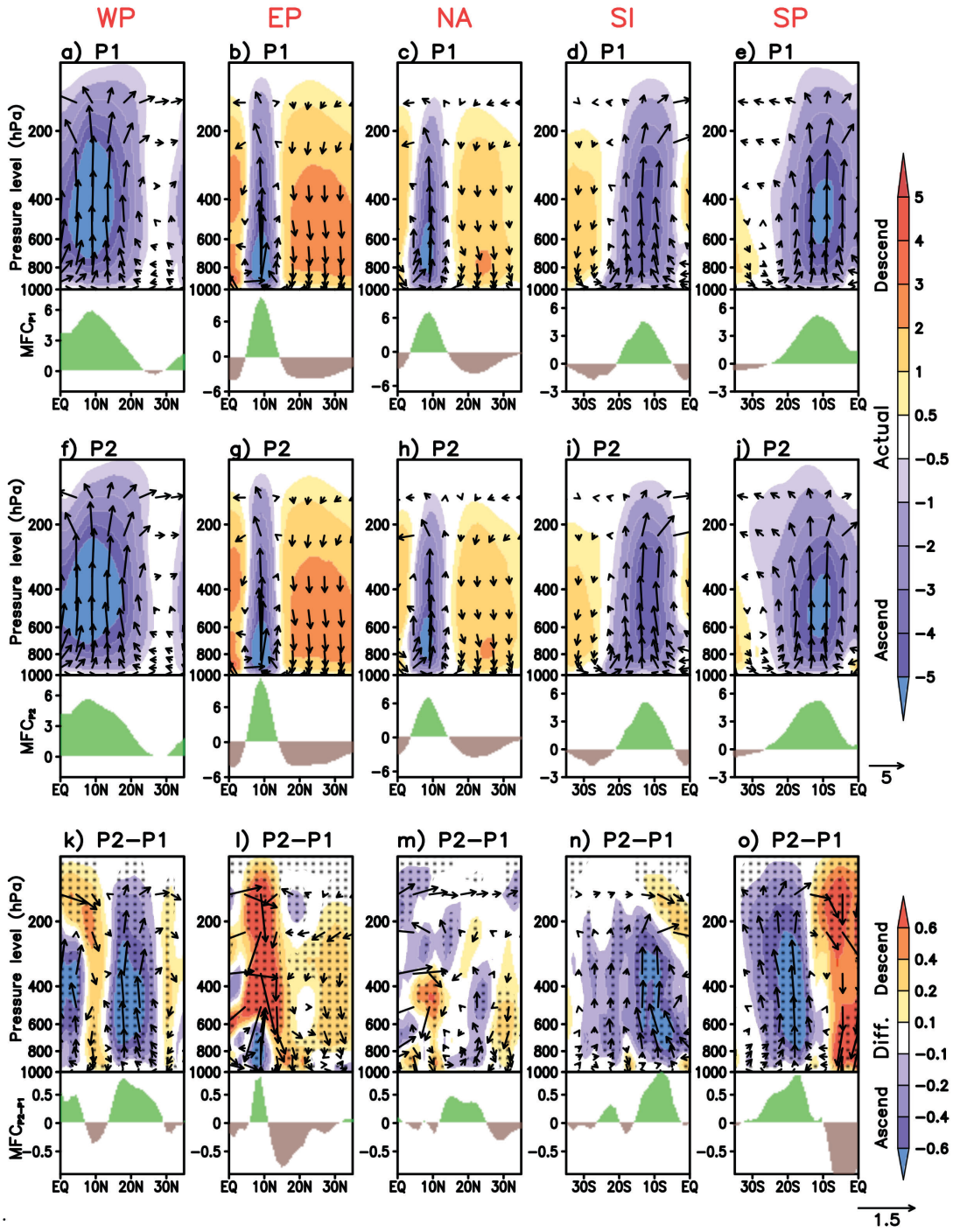

Meridional-vertical distribution of the longitudinally averaged divergent meridional wind and vertical pressure velocity (in vector) based on ERA-Interim[32] datasets: **a-e**, pre-1998 period (P1). **f-j**, post-1998 period (P2) and **k-o**, epochal changes (P2-P1). The vertical pressure velocity (omega, $\times 10^{-2}$ hPa s^{-1}) averaged over the same domain is also shown in colour shading. Black dots denote values statistically significant at the 95% confidence level. The meridional distribution of the moisture flux convergence (MFC) are also shown (in shaded) at the bottom of each panel.

Note that the poleward shift of the regional HC is markedly prominent over the western north Pacific (Fig. 4k), south Pacific (Fig. 4o) and south Indian (Fig. 4n), particularly where the seasonal monsoon trough exists. Such a shift is however weaker over the eastern north Pacific (Fig. 4l) and rather absent in the north Atlantic (Fig. 4m), although an anomalous poleward shift of the actual position of the climatological subtropical dry zone is relatively prominent. The corresponding meridional changes in low-level (surface – 700hPa) integrated large-scale moisture flux convergence (MFC) conducive for TCG[10] (Fig. 4, bottom panel) also capture a similar meridional shift, except over the eastern Pacific, where the TCG is predominantly modulated by enhanced vertical wind shear (+40%) collocated with a large increase in the vertical stability in the post-1998 epoch.

Our results highlight a possible new dynamical link between the recent tropical expansion and altered behaviour of TCG, emphasizing the indirect influence of ongoing global warming. Although there are regional differences in the results, most basins exhibit low-latitude reduction and poleward expansion in preferred TCG regions tied with the dynamic suppressing effect from the poleward expanding regional HC, partly linked with the enhanced vertical stability and an associated decrease in the HC strength at upper levels. Thus, the HC perspective unifies both the large-scale dynamic and thermodynamic conditions impacting regional TCG, and thus provides a new framework to quantify and understand the mechanisms behind the recent and future changes in TCG via the warming-induced climate pathways of tropical expansion.

Owing to the limited accuracy of many historical TC records before the 1980's, our results are constrained by data limitations in determining the TC trends and in clarifying the fundamental

processes that drive the HC changes and their relationship with global climate change. The observed relationship between the changes in TCG and tropical expansion may be clearer in future decades as more observations become available and the signal from the climate change forcing becomes more prominent. In the meantime, climate model experiments could give some guidance on the physical mechanisms behind this relationship. Note that the latest CMIP5 climate models could not reproduce the apparently observed changes in the HC, and also have low confidence in projecting in tropical cyclone genesis-location, tracks, duration or areas of impacts[6]. Given the potential societal impact of a future poleward shift in typical regions of TC formation, this relationship merits further investigation.

Methods.

Data. Observed TCs are from 6-hrly global TC best-track data (IBTrACS-WMO, v03r09; ref 29, https://www.ncdc.noaa.gov/ibtracs). Climate variables analyzed are extracted from the ERA-Interim Reanalysis (ref. 31; http://apps.ecmwf.int/datasets) of resolution 1.5° × 1.5°. The monthly Extended Reconstructed SST (ERSSTv4; ref. 34) of resolution 2° × 2° is also used (http://www.ersl.noaa.gov/psd/).

Domain and Definition of TCG frequency. The TC best track dataset is grouped into five TC active ocean basins, namely western Pacific (WP), eastern Pacific (EP), north Atlantic (NA), south Indian (SI) and south Pacific (SP) (Supplementary Fig 1) within the tropical domain (30°S to 30°N). We have excluded the north Indian Ocean basin because TCs are infrequently labelled before 1990 in this best-track version. The TCG frequency is defined as the number of tropical storms that exceed maximum wind of 33 knots. The location of TCG is identified based on the position of the tropical storms at which the maximum wind speed exceeds 33 knots, and TCG distribution is computed per 2°×2° grid box per peak season. Peak TC seasons of each basin are selected based maximum TC

activity, which typically occur during July to October (JASO) in the WP, July to September (JAS) in the EP, August to October (ASO) for the NA, and January to March (JFM) for both the SI and SP. Nearly 70% of all TCs form during the peak TC season in almost all basins[10].

Climate diagnostics.

Maximum potential intensity (MPI). It is the theoretical maximum intensity that TCs could reach under specific environmental conditions over the deep tropics , and is often considered relevant to quantify TC activity. Here the MPI (Fig. 2) is calculated based on Emanuel's study[34],

$$MPI = \frac{T_s}{T_o}\frac{C_k}{C_D}\left[CAPE_e - CAPE_b\right] \quad (1)$$

where T_s is the SST, T_0 is the mean outflow temperature, C_k is the exchange coefficient for enthalpy, and C_D the drag coefficient. The quantity $CAPE_e$ is the convective available potential energy with reference to the environmental sounding, and $CAPE_b$ is that of boundary layer air.

Moisture flux convergence (MFC). Calculated based on a recent study[10], the low-level (surface to 700hPa) integrated MFC (Fig. 4, bottom panel) is an important TC-favourable large-scale condition that combines both the effects of large-scale converging winds and moisture advection important for TCG variation.

$$MFC \equiv -\frac{1}{\rho_w g}\int_{700}^{sfc} \nabla \cdot \boldsymbol{V}q \, dP \quad (2)$$

where ρ_w is the density of water, V is the wind vector and q is the specific humidity.

Atmospheric stability. The atmospheric dry static stability (Fig. 1b) is defined as the potential temperature (θ) difference between upper (300 hPa) and lower (900hPa) level of the atmosphere. Alternately, the vertical moist stability (VMS) is introduced to represent the atmospheric convective stability over tropics at regional scales. It is derived as the difference between vertically integrated upper (200-500hPa) and lower (1000-700hPa) layers of total moist static energy (MSE).

$$VMS = MSE_{\text{upper<200-500hPa>}} - MSE_{\text{lower<1000-700hPa>}} \quad (3)$$

$$MSE = C_pT + gz + L_vq \qquad (4)$$

where Cp is the specific heat at constant pressure, T is the absolute air temperature, g is the gravitational constant, z is the height above the surface, Lv is the latent heat of vaporization and q is the specific humidity. The vertical integral $\langle\cdot\rangle$ denotes a mass integration through the upper and lower vertical levels.

Mean Meridional Circulation. The mean meridional circulation is a zonal-mean quantity defined for axisymmetric two-dimensional flow. The Stokes streamfunction (ψ) is commonly used to study the strength and geometry of the HC. In this approach, the mean meridional circulation is assumed to be non-divergent, i.e. the conservation of mass should satisfy the conditions at the vertical pressure coordinate:

$$\frac{1}{a}\frac{\partial[v]}{\partial\phi} + \frac{\partial[\omega]}{\partial p} = 0 \qquad (5)$$

where v is the meridional velocity, ω is the pressure vertical velocity and $[\cdot]$ denotes the zonal mean. (5) indicates that $[v]$ or $[\omega]$ can be used to define the two-dimensional flow. Based on (5) the Stokes streamfunction (ψ) can be defined as,

$$[v] = \frac{g}{2\pi a cos\phi}\frac{\partial\psi}{\partial p} \quad (6) \quad \text{and} \quad [\omega] = -\frac{g}{2\pi a^2 cos\phi}\frac{\partial\psi}{\partial\phi} \quad (7)$$

where ϕ is the latitude, and p is the pressure, g is the acceleration due to gravity.

Here, the streamfunction $\psi(\phi, p)$ is calculated based on $[v]$, where the value of ψ at a given latitude and pressure level equals to the rate of meridional mass transport (Fig. 3):

$$\psi(\phi, p) = \frac{2\pi a cos\phi}{g}\int_0^p [v]\, dp \qquad (8)$$

Note that the assumption of non-divergent meridional circulation is valid over the global domain where $\psi(\phi, p)$ must satisfy the Equation 5; however, this condition is not satisfied over a limited longitudinal band, e.g. 120˚-180˚E where ($\int_{120E}^{180E}\frac{\partial u}{\partial x}\, dx \neq 0$) at all latitudes, and therefore may not be useful to represent regional HC over individual TCG domains. To overcome this limitation,

the zonal-mean divergent component of the meridional flow (v_ϕ) can be regarded as part of the meridional overturning circulation, i.e. the Hadley circulation.

Statistical significance. We have used a two-sided Student's t-test at the 95% significance level.

CMIP5 climate models. Projection of future changes in the Hadley circulation is assessed using a multi-model mean of 13 CMIP5 climate models[31] (listed in supplementary Table ST1). The simulations from historical (1980-2005) and RCP8.5 (2060-2095) experiments are analyzed. The historical runs (20th century simulations) are forced by observed transient climate forcing from the instrumental period. The RCP8.5 runs (21st century simulations) are forced with relatively high anthropogenic GHGs emissions designed so that anthropogenic radiative forcing will increase and then stabilize at ~8.5Wm-2 after 2100. CMIP5 model output is available from the Earth System Grid Federation (ESGF) (https://esgf-node.llnl.gov/projects/cmip5).

Reference

1. Peduzzi, P. et al. Global trends in tropical cyclone risk. *Nat. Clim. Change* 2, 289-294 (2012).
2. Gray, W. Hurricanes: Their formation, structure and likely role in the tropical circulation. *Meteorology Over Tropical Oceans. D. B. Shaw (Ed.), Roy. Meteor. Soc., James Glaisher House, Grenville Place, Bracknell, Berkshire, RG12 1BX,* pp.155-218 (1979).
3. Sharmila, S. & Walsh, K. Impact of Large-scale Dynamical versus Thermodynamical Climate Conditions on Contrasting Tropical Cyclone Genesis Frequency. *J. Clim.* (2017). doi:10.1175/jcli-d-16-0900.1
4. Defforge, C. & Merlis, T. Observed warming trend in sea surface temperature at tropical cyclone genesis. *Geophys. Res. Lett.* 44, 1034-1040 (2017).
5. Dare, R. & McBride, J. The Threshold Sea Surface Temperature Condition for Tropical Cyclogenesis. *J. Clim.* 24, 4570-4576 (2011).
6. Knutson, T. et al. Tropical cyclones and climate change. *Nat. Geosci.* 3, 157-163 (2010).

7. Emanuel, K. Increasing destructiveness of tropical cyclones over the past 30 years. *Nature* 436, 686-688 (2005).
8. Webster, P. Changes in Tropical Cyclone Number, Duration, and Intensity in a Warming Environment. *Science* 309, 1844-1846 (2005).
9. Grossmann, I. & Morgan, M. Tropical cyclones, climate change, and scientific uncertainty: what do we know, what does it mean, and what should be done? *Climatic Change* 108, 543-579 (2011).
10. Walsh, K. et al. Tropical cyclones and climate change. *Wiley Interdisciplinary Reviews: Climate Change* 7, 65-89 (2015).
11. Kossin, J., Emanuel, K. & Vecchi, G. The poleward migration of the location of tropical cyclone maximum intensity. *Nature* 509, 349-352 (2014).
12. Kossin, J., Emanuel, K. & Camargo, S. Past and Projected Changes in Western North Pacific Tropical Cyclone Exposure. *J. Clim.* 29, 5725-5739 (2016).
13. Li, T. et al. Global warming shifts Pacific tropical cyclone location. *Geophys. Res. Lett.* 37, n/a-n/a (2010).
14. Murakami, H. et al. Future Changes in Tropical Cyclone Activity Projected by the New High-Resolution MRI-AGCM*. *J. Clim.* 25, 3237-3260 (2012).
15. Walsh, K.E. et al. Hurricanes and climate: the U.S. CLIVAR working group on hurricanes. *Bull. Am. Meteorol. Soc.* 96, 997–1017 (2015).
16. Daloz, A.S. & Camargo, S.J. Is the poleward migration of tropical cyclone maximum intensity associated with a poleward migration of tropical cyclone genesis? *Clim Dyn* (2017). https://doi.org/10.1007/s00382-017-3636-7
17. Emanuel, K. Tropical cyclone activity downscaled from NOAACIRES reanalysis. *J. Adv. Model. Earth Syst*., 2, 1, 1908–1958 (2010).

18. Camargo, S.J., Tippett, M.K., Sobel, A.H., Vecchi, G.A., Zhao, M. Testing the performance of tropical cyclone genesis indices in future climates using the HIRAM model. *J. Clim.* 27, 9171–9196 (2014).

19. Lucas, C., Timbal, B. & Nguyen, H. The expanding tropics: a critical assessment of the observational and modeling studies. *WIREs. Clim. Change* 5, 89–112 (2014).

20. Hu, Y. & Fu, Q. Observed poleward expansion of the Hadley circulation since 1979. *Atmos Chem Phys* 7, 5229–5236 (2007).

21. Polvani, L.M., Waugh, D.W., Correa, G.J.P., Son, S-W. Stratospheric ozone depletion: the main driver of twentieth-century atmospheric circulation changes in the Southern Hemisphere. *J. Clim.* 24:795–812 (2011).

22. Quan, X.-W. et al. How fast are the tropics expanding? *J. Clim* 27, 1999– 2013, (2014).

23. Lu, J., Vecchi, G. A. & Reichler, T. Expansion of the Hadley cell under global warming. *Geophys. Res. Lett*. 34, L06805 (2007).

24. Knutson, T., and S. Manabe, 1995: Time-mean response over the tropical pacific to increased CO2 in a coupled ocean–atmosphere model. *J. Clim*, 8, 2181–2199.

25. Vecchi, G. A., & Soden, B. J. Global warming and the weakening of the tropical circulation. *J. Clim.* 20, 4316–4340 (2007).

26. Gastineau, G., Le Treut, H. & Li, L. Hadley circulation changes under global warming conditions indicated by coupled climate models. *Tellus* 60A, 863–884 (2008).

27. Santer, B. D. et al. Tropospheric warming over the past two decades. *Scientific Reports* 7, 2336 (2017).

28. Xiang, B., Wang, B., Lauer, A. et al. Upper tropospheric warming intensifies sea surface warming. *Clim Dyn* 43: 259 (2014).

29. Knapp, K. R., Kruk, M. C., Levinson, D. H., Diamond, H. J., and Neumann, C. J. The International Best Track Archive for Climate Stewardship (IBTrACS) unifying tropical cyclone data. *Bull. Amer. Meteor. Soc.* 91, 363–376 (2010).
30. Emanuel, K. The maximum intensity of hurricanes. *J. Atmos. Sci*. 45, 1143–1155 (1988).
31. Dee, D. P., et al. The ERA-Interim reanalysis: Configuration and performance of the data assimilation system. *Quart. J. Roy. Meteor. Soc.* 137, 553–597 (2011).
32. Mbengue, C., & Schneider, T. Storm track shifts under climate change: What can be learned from large-scale dry dynamics. J. Clim 26, 9923–9930 (2013).
33. Taylor, K. E., Stouer, R. J. & Meehl, G. A. An overview of CMIP5 and the experimental design. *Bull. Am. Meteorol. Soc*. 93, 485498 (2012).
34. Huang, B., et al. Extended Reconstructed Sea Surface Temperature version 4 (ERSST.v4). Part I: Upgrades and intercomparisons. *J. Clim* 28, 911–930 (2014).

Acknowledgement. This research was undertaken with the assistance of resources from the National Computational Infrastructure (NCI), supported by the Australian Government. We also grateful to the World Climate Research Programme's Working Group on Coupled Modelling and the climate modelling groups for producing and making available their model output. S.S. is supported by Australian Research Council Discovery Project (DP150102272). S.S acknowledges Prof. K. Emanuel, Prof. S. Camargo and Dr. H. Hendon for valuable discussions.

Contributions. S.S. conceived the study, and performed the analysis in discussion with K.J.E.W. Both the authors discussed the results and jointly contributed in writing the manuscript.

Competing financial interests. The authors declare no competing financial interests.